Food Hydrocolloids 31 (2013) 85–93

Contents lists available at SciVerse ScienceDirect

Food Hydrocolloids

journal homepage: www.elsevier.com/locate/foodhyd

Formation and dynamic interfacial adsorption of glycinin/chitosan soluble complex at acidic pH: Relationship to mixed emulsion stability

Yang Yuan [a], Zhi-Li Wan [a], Shou-Wei Yin [a], Zi Teng [b], Xiao-Quan Yang [a,*], Jun-Ru Qi [a], Xiao-Ying Wang [c]

[a] Research and Development Center of Food Proteins, College of Light Industry and Food, South China University of Technology, Guangzhou 510640, PR China
[b] Department of Nutrition and Food Science, 0112 Skinner Building, University of Maryland, College Park, MD 20742, United States
[c] Key Laboratory of Pulp & Paper Engineering, College of Light Industry and Food, South China University of Technology, Guangzhou 510640, PR China

ARTICLE INFO

Article history:
Received 20 April 2012
Accepted 8 October 2012

Keywords:
Glycinin
Chitosan
Complex
Interface
Emulsion

ABSTRACT

The formation and interfacial adsorption of glycinin/chitosan (CS) soluble complex were investigated at acidic pH. The stability of the mixed emulsion stabilized by the complex was also evaluated at pH 4.5. Turbidimetric analysis, isothermal titration calorimetry (ITC) and dynamic light scattering were used to characterize the dynamic formation of the complex. The results showed that soluble complexes were formed mainly at pHs between 4.0 and 6.0, depending on CS/Glycinin mixing ratio. At pH 4.5, soluble complex was formed and saturated at mixing ratio = 0.1, showing a maximum size distribution at 164.2 nm. We found that the glycinin/CS soluble complex showed improved interfacial adsorption than glycinin at pH 4.5. In detail, dynamic interfacial adsorption data showed the coefficient of diffusion (K_{diff}), unfolding (K_1) and rearrangement (K_2) for soluble complex (K_{diff}, K_1 and K_2: 0.58 mNm^{-1} $s^{-0.5}$, 2.23 E−4 s^{-1} and 5.78 E−4 s^{-1}) were higher than those of the glycinin (K_{diff}, K_1 and K_2: 0.32 mNm^{-1} $s^{-0.5}$, 1.72 E−4 s^{-1} and 4.63 E−4 s^{-1}). The droplet size and confocal observation of the mixed emulsion fabricated with glycinin/CS soluble complex displayed improved stability at mixing ratios of 0.1 to/and 0.2, suggesting the synergistic effect of the two molecules. We concluded that interfacial and emulsifying properties of glycinin could be improved by formation of glycinin/CS soluble complex at acidic pH.

1. Introduction

Nowadays, mixed systems of proteins and polysaccharides are widely used in food industry. The exploitation of protein/polysaccharide interactions offers opportunities for the design of new ingredients with application (Dickinson, 2008). In general, the interactions between proteins and polysaccharides can be either segregative or associative. Phase behavior, microstructure and rheology of segregative interaction have been studied extensively (Çakır & Foegeding, 2011; Farouk, Frost, Krsinic, & Wu, 2011; Zhu et al., 2008). In recent years, research has been focused on the protein/polysaccharide associative interaction (Schmitt & Turgeon, 2011; Turgeon, Schmitt, & Sanchez, 2007). In this case, the complexation of protein and polysaccharide can lead to the formation of soluble and insoluble complexes, depending on the colloidal properties of the protein/polysaccharide systems (Anal, Tobiassen, Flanagan, & Singh, 2008; Ye, Flanagan, & Singh, 2006).

Although the complexation between protein and polysaccharide has been reported in a number of literature, most of them were focused on anionic polysaccharides (Turgeon et al., 2007; Ye et al., 2006). Chitosan (CS) [(1-4)-2-amino-2-deoxy-β-D-glucan] is a linear cationic polysaccharide, and it has been widely employed in food, agricultural and biomedical industries, owing to its non-toxicity, biocompatibility and antibacterial properties (Borges et al., 2006; No, Park, Lee, & Meyers, 2002). At acidic pH values (pH < 6), chitosan can interact with negatively charged proteins or polysaccharides to form either soluble or insoluble complexes. Recently, the complex between milk protein (e.g., bovine serum albumin, whey protein isolates and β-lactoglobulin) and chitosan was investigated. The effects of pH, mixing ratio, NaCl content and thermal treatment on the complexation were studied for better understanding the mechanisms of the associative interaction (Anal et al., 2008; Guzey & McClements, 2006; Hong & McClements, 2007; Mounsey, O'Kennedy, Fenelon, & Brodkorb, 2008; Souza, Bai, Gonçalves, & Bastos, 2009; Souza, Gonçalves, & Gómez, 2011; Vardhanabhuti, Yucel, Coupland, & Foegeding, 2009).

In comparison, the complexation between chitosan and vegetable proteins (such as soy protein) was seldom investigated, probably due to the complicated structure of these proteins.

* Corresponding author. Tel.: +86 20 87114262; fax: +86 20 87114263.
E-mail addresses: fexqyang@163.com, fexqyang@scut.edu.cn (X.-Q. Yang).

0268-005X/$ – see front matter © 2012 Elsevier Ltd. All rights reserved.
http://dx.doi.org/10.1016/j.foodhyd.2012.10.003

Takeuchi, Morita, Saito, Kugimiya, and Fukamizo (2006) indicated the thermal stability of soy β-conglycinin at acidic pH was improved by interacting with chitosan electrostatically. Liu, Yang, et al. (2011) and Liu, Zhao, Liu, & Zhao, 2011 discussed the light scattering properties of soy globulin/chitosan complexes under hydrothermal conditions as a function of pH. Elmer, Karaca, Low, and Nickerson (2011) investigated the complex coacervation in pea protein isolate–chitosan mixtures by a turbidimetric analysis during pH titration.

To our knowledge, no studies have been carried out on relationship between the soy protein/chitosan complex formation, interfacial properties and emulsion stability. Laplante, Turgeon, and Paquin (2005a, 2005b, 2006) investigated the effect of chitosan on whey protein emulsion stability as influenced by pH, mixing ratio, ionic strength and various chitosan. Even in other protein/polysaccharide system, these kinds of studies are also much less than the investigation about the mechanism of interaction. Liu et al. (2012) found the relationship between the emulsion stability of sodium caseinate/carboxymethylcellulose and their interactions at oil–water interface. Gharsallaoui, Yamauchi, Chambin, Cases, and Saurel (2010) indicated that the pectin induced emulsion stability of pea protein could be mainly assigned to steric repulsion and interfacial membrane rigidity improvement after pectin adsorption.

Soy proteins are the most important representatives of legume proteins. However, the effect of chitosan on the soy protein/chitosan complex formation, interfacial properties and emulsion stability is hardly known. Glycinin is the most important storage protein of soybean and is a globular protein. It consists of two polypeptide components linked via disulfide bonds (AB), one (A, $M_w = 34–44$ kDa) with acidic and the other (B, $M_w = 20$ kDa) with basic isoelectric points (Staswick, Hermodson, & Nielsen, 1981). These subunits were suggested to assemble into a hexamer [$(AB)_6$] by previous literature. At certain pHs and ionic strengths, glycinin (11S) dissociates into the 7S form [$(AB)_3$] and/or the 3S form (AB) (van Vliet, Martin, & Bos, 2002). Such dissociation is mainly driven by electrostatic repulsion (Martin, Bos, & van Vliet, 2002). The aim of this study was to illuminate the formation of glycinin/CS soluble complexes in aqueous mixtures and its effect on the stability of mixed emulsions at acidic pHs. The formation, interfacial adsorption, emulsion stability and microstructure of glycinin/CS soluble complexes were investigated. The study can be an available reference for the utilization of chitosan in soybean-based food (e.g., soybean milk and soybean beverages).

2. Materials and methods

2.1. Materials

The defatted soybean flakes were purchased from Shandong Xinjiahua Industrial & Commercial Co. Ltd., China. The protein content of soy flour was 55.0 ± 0.5% (determined by Kjeldahl method with nitrogen conversion factor of 6.25; on dry basis) and nitrogen solubility index 83.6 ± 0.6%. Chitosan (molecular weight about 300 kDa, degree of deacetylation 95%) was purchased from Shandong Aokang Industrial & Commercial Co. Ltd., China. Corn oil was purchased from local supermarket in Guangzhou. All chemicals used in this work were of analytical or better grade.

2.2. Preparation of glycinin

The glycinin was prepared according to the Nagano's procedure (Nagano, Hirotsuka, Mori, Kohyama, & Nishinari, 1992). Soybean defatted flakes were ground and sieved (60 mesh size). The protein was extracted by making slurry with 15-fold volumes of deionized water and adjusted to pH 7.5 with 2 N NaOH at room temperature for 2 h with stirring. This slurry was put through a nylon mesh (180 mesh size) and the filtrate was collected and centrifuged at 9000 g (CR22G High-Speed Refrigerated Centrifuge, HITACHI, Japan) for 30 min. After dry sodium bisulfite (SBS) was added to the supernatant (0.98 g of SBS/L), the pH was adjusted to 6.4 with 2 N HCl. The mixture was kept in ice bath overnight and then centrifuged (6500 g × 20 min) at 4 °C. The precipitate (glycinin fraction) was washed twice with deionized water before suspended with minimum volumes of deionized water and adjusted to pH 7.5 with 2 N NaOH. The supernatant was dialyzed three times at 4 °C against deionized water (1:10 times), and then lyophilized to yield the glycinin fraction. Protein content of this lyophilized powder was 93.6 ± 0.9% determined by the Dumas method ($N \times 6.25$).

2.3. Preparation of aqueous mixtures

Glycinin (2%, w/v) and chitosan (2%, w/v) stock solutions were prepared by dissolving the powders in 100 mM acetic acid/sodium acetate buffer (pH 3.0) with stirring (600rpm) at room temperature for 3 h. The glycinin/CS mixture was obtained by mixing two stock solutions. Various concentrations of mixtures were obtained by diluting the mixtures with acetic acid/sodium acetate buffer at the desired pH and ionic strength (NaCl). The concentration of the glycinin set at constant (5 mg/mL) and the mixing ratio of chitosan to glycinin (CS/Glycinin) was set from 0.05 to 0.8 (w/w).

2.4. Preparation of mixed emulsion

The aqueous glycinin/chitosan emulsifier solutions (Glycinin, 5 mg/mL) were obtained by diluting the mixtures with 100 mM acetic acid/sodium acetate buffer at pH 4.5. Then, these solutions were emulsified with corn oil using an Ultra-turrax (T25, IKA, Staufen, Germany) at 10,000 r/min for 2 min. Finally, the coarse emulsions were passed through a homogenizer (Microfluidizers M-110 EH Processor Co., Lampertheim, Germany) at 400 bar pressure for twice passes. In all the final emulsions, the oil/glycinin ratio was 20:1 (w/w). The emulsions were stored at 4 °C prior to further analysis.

2.5. Turbidimetric analysis during a base titration

Mixtures of protein and polysaccharide form an electrostatic complex in a specific pH range. The phase boundaries (pH_c, pH_φ) were determined by using an original titration method. Base titration of the mixture (Glycinin, 5 mg/mL) during turbidimetric analysis was achieved through the addition of 1 M NaOH. Change of turbidity was measured as a function of pH (3.0–8.0) using a Genesys 10 visible-ultraviolet spectrophotometer (Thermo Scientific, Waltham, MA) at 600 nm.

2.6. Dynamic light scattering, electrophoretic light scattering & laser light scattering measurement

The dynamic light scattering and electrophoretic light scattering measurements were performed with a Nanosizer ZS instrument (Malvern Instruments Ltd., Worcestershire, UK), while laser light scattering was measured using a Malvern Mastersizer 2000 unit (Malvern Instruments Ltd., Worcestershire, UK). The size distribution of the mixture was measured using a dynamic light scattering (DLS) method in this research, and it was calculated from the speed of the light intensity fluctuation (Jourdain, Leser, Schmitt, Michel, & Dickinson, 2008). All determinations were conducted in triplicate.

The ζ-potential of the mixture (Glycinin 5 mg/mL) and mixed emulsion (Oil concentration, 1 mg/ml) were measured by laser

Doppler velocimetry (Jourdain et al., 2008). It was assumed that the dielectric constant and viscosity of the aqueous solution surrounding the particles was the same as that of pure buffer, which is a reasonable assumption for low biopolymer concentrations. All determinations were conducted in triplicate.

Droplet size of the emulsions was determined by laser light scattering. The droplets were characterized under high dilution conditions by dispersing the samples in an acetic acid/sodium acetate buffer-filled tank at pH 4.5. The refractive indices of water and corn oil were taken as 1.330 and 1.520, respectively. The mean droplet size was characterized in terms of the volume mean diameter D_{43}. All measurements were conducted in duplicate.

2.7. Isothermal titration calorimetry (ITC)

The energetics of the interaction between chitosan and glycinin were measured using an isothermal titration calorimeter (VP-ITC, MicroCal, Northampton, MA) with a reaction cell volume of 1.4437 mL. The glycinin solution (1 mg/mL) was loaded into the calorimetric cell, equilibrated at 25 °C, and titrated adding 30 successive 5 μL injections of CS (1 μg/μL) while continuously stirring the solution at 600 rpm. Each injection lasted 10 s, and there was an interval of 180 s between successive injections. Control titrations were performed to obtain the heat of dilution by injecting the chitosan solution into the acetic acid/sodium acetate buffer without counterpart. The data were acquired by the software developed by MicroCal. Measurements were carried out in duplicate, and the results are reported as the mean.

2.8. Dynamic interfacial adsorption

The dynamic interfacial adsorption of the mixture at the oil–water interface was determined by monitoring the evolution of surface pressure (π) with time (θ). The samples were diluted to 1 mg/mL (Glycinin) with 100 mM acetic acid/sodium acetate buffer at pH 4.5 to minimize the influence of aggregation. An optical contact angle meter, OCA-20, with oscillating drop accessory ODG-20 (Dataphysics Instruments GmbH, Germany) was used in a dynamic mode for measuring surface pressure (π) at the oil–water interface at 25 °C. Details of this apparatus are given elsewhere (Caseli, Masui, Furriel, Leone, & Zaniquelli, 2005). The sample solutions were placed in the syringe to reach the desired constant temperature. Then a drop was delivered into a purified corn oil and allowed to stand for 3 h to achieve protein adsorption. Measurements were made at least twice. The average standard accuracy of the surface pressure was roughly 0.2 mN/m.

2.9. Confocal Laser Scanning Microscope (CLSM)

CLSM-images of the selected mixture were recorded at room temperature with a Leica TCS SP5 Confocal Laser Scanning Microscope (Leica Microsystems Inc., Heidelberg, Germany), equipped with an inverted microscope (Model Leica DMI6000). The images were captured in the single photon mode with an Ar/Kr visible light laser. Before imaging, the mixed emulsion (Protein, 5 mg/mL; Oil, 100 mg/mL) were mixed with Nile Blue–Nile Red mixed solution (30 μL of a 1 wt % Nile Blue and 0.2 wt % Nile Red solution per mL sample). After that, a drop of the stained mixture was placed on a concave slide, which was then covered with a glycerol-coated cover slip. The wavelengths of the incident lights were 488 nm and 633 nm for Nile Red and Nile Blue, respectively. The fluorescence light was recorded between suitable wavelengths. Leica objective lenses of 100 × magnification were used. Digital image files were acquired in 1024 × 1024 pixel resolution. Generally, images were recorded with the 100 × objective lens. Z-stacks of xyscans were recorded between 5 μm and 45 μm penetration, with an interval of 2 μm. The reported images were recorded at a penetration depth of 15 μm. This depth avoided artefacts that occur close to the glass slide and resulted in representative images.

2.10. Statistical analysis

All the data were subjected to one way analysis of variance and correlations between the result were carried out using Statistical Analysis System Software (SAS version 9.0, SAS Institute, Cary, NC); significant differences were determined by Duncan's multiple range test and accepted at $p < 0.05$ (Duncan, 1955).

3. Results and discussion

3.1. Aqueous mixtures

3.1.1. Phase diagrams of turbidimetric analysis

Protein and polysaccharide formed an electrostatic complex in a specific pH range. Critical pH values associated with the formation of soluble (pH_c) and insoluble (pH_φ) complexes were determined graphically as the intersection point of two curve tangents (Elmer et al., 2011; Weinbreck, de Vries, Schrooyen, & de Kruif, 2003). According to Fig. 1, as pH was increased, glycinin and chitosan formed soluble complex when the first boundary pH (pH_c) was reached. When pH continued to increase to a second boundary value (pH_φ), the interaction between the two molecules became stronger, leading to phase separation. The investigation of phase boundaries was to select suitable pHs for the formation of glycinin/CS soluble complex.

Fig. 2A shows that the pH_c and pH_φ increased significantly ($p < 0.05$) with increased concentrations of chitosan. In detail, all samples showed no complexation at pHs below 4.0, and soluble complexes were found mainly between pH 4.0 and 6.0, depending on mixing ratio. Furthermore, the increase in pH_φ was more prominent than that of pH_c, suggesting that the formation of insoluble complex (coacervate) was influenced more significantly by the mixing ratio (Fig. 2A). Similar results were presented by Anal who reported the soluble caseinate–chitosan complexes were obtained in the pH range 4.8–6.0 (Anal et al., 2008). The difference of phase boundaries may be related to the native properties of different protein. Concomitantly, the ζ-potential at pH_c was dependent on the biopolymer mixing ratio ($p < 0.05$), whereas the

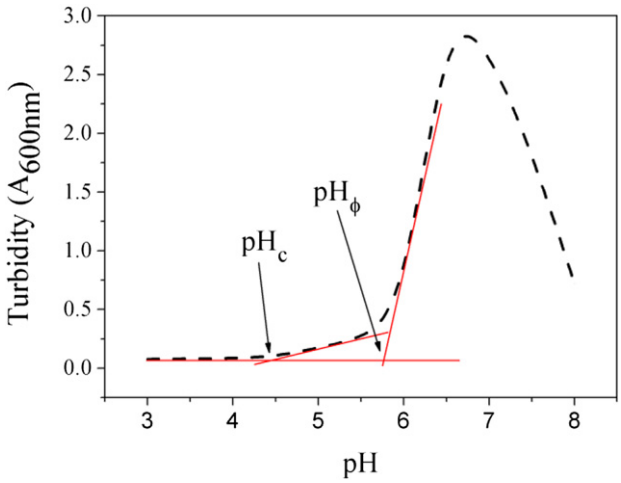

Fig. 1. Mean turbidity profile as a function of pH for CS/Glycinin mixing ratio of 0.2, showing the graphical interpretation of pH-induced structure forming events associated with the formation of soluble (pH_c) and insoluble (pH_φ) complexes.

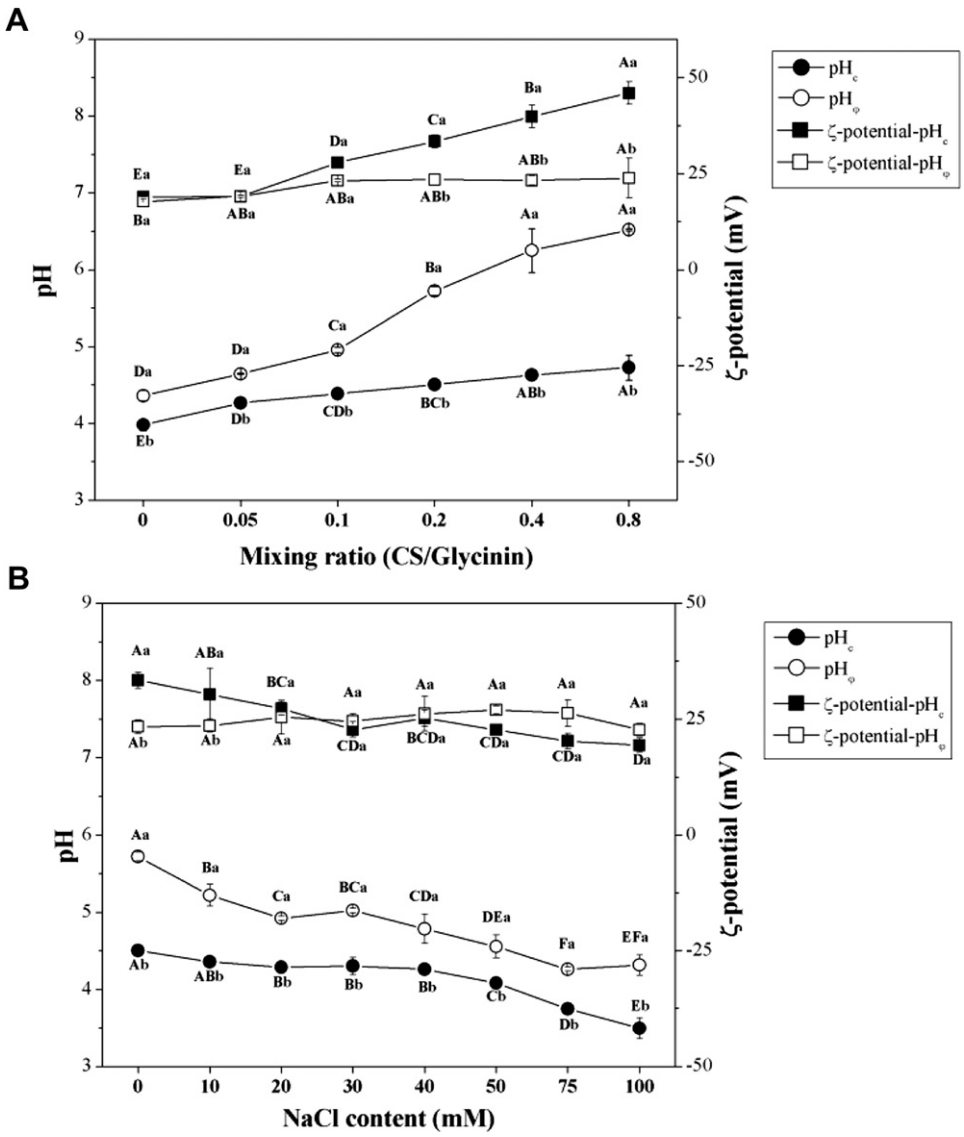

Fig. 2. Phase boundaries (pH_c, pH_φ) and ζ-potential at phase boundaries of glycinin/chitosan (CS) mixtures as function of (A) CS/Glycinin mixing ratio (From 0 to 0.8, NaCl content = 0 mM) and (B) NaCl content (From 0 to 100 mM, CS/Glycinin mixing ratio = 0.2).

ζ-potential at pH_φ was ratio independent. At all mixing ratios, ζ-potential of mixtures always carried net positive charge at pH_c and pH_φ. Moreover, at mixing ratios higher than 0.1, the ζ-potential at pH_c was higher than that at pH_φ. This phenomenon could be ascribed to the effect of surplus chitosan in mixtures (Weinbreck et al., 2003).

Fig. 2B highlights the strong effect of sodium chloride (NaCl) concentration on complex formation. The addition of NaCl (10–100 mM) caused a significant decrease of the pH_c from 4.5 to 3.5 and pH_φ from 5.7 to 4.3, respectively ($p < 0.05$). The presence of NaCl resulted in increased ionic strength, which was known to reduce and suppress the electrostatic complexation owing to its screening effect on the charged groups of the polymers. Based on our results, glycinin/chitosan complexation was probably electrostatically driven. This indication was corroborated by the fact that the ζ-potential at pH_c was significantly reduced by the addition of NaCl (Fig. 2B). More interestingly, it can be found that, at the same NaCl concentration (began from 30 mM), the ζ-potential at pH_φ was even slightly higher than at pH_c, although it is not significant. This phenomenon can be also ascribed to the electrostatic screening of the NaCl.

3.1.2. The formation of glycinin/CS soluble complex

According to the results in the previous section, pHs 3.5 and 4.5 were selected for further investigating the formation of glycinin/CS soluble complex (Fig. 3). The heat flow versus time profiles were obtained for chitosan solution titrated into glycinin solution at pHs 3.5 and 4.5. As is shown in Fig. 3A, the corrected heat flow at pH 4.5 decreased as the content of chitosan increased. This result implied the existence of affinity binding sites. At pH 3.5, the corrected heat flow induced by the binding was too small to be measured (Fig. 3B). This could be attributed to the fact that both glycinin and chitosan were positively charged at pH 3.5, so there should not be electrostatic attraction between them. Similar results were observed for the complexation between β-lactoglobulin and chitosan in aqueous solution (Guzey et al., 2006). At pH 4.5, the formation of glycinin/CS complex was characterized by an exothermic enthalpy change. The ΔH initially exhibited a large

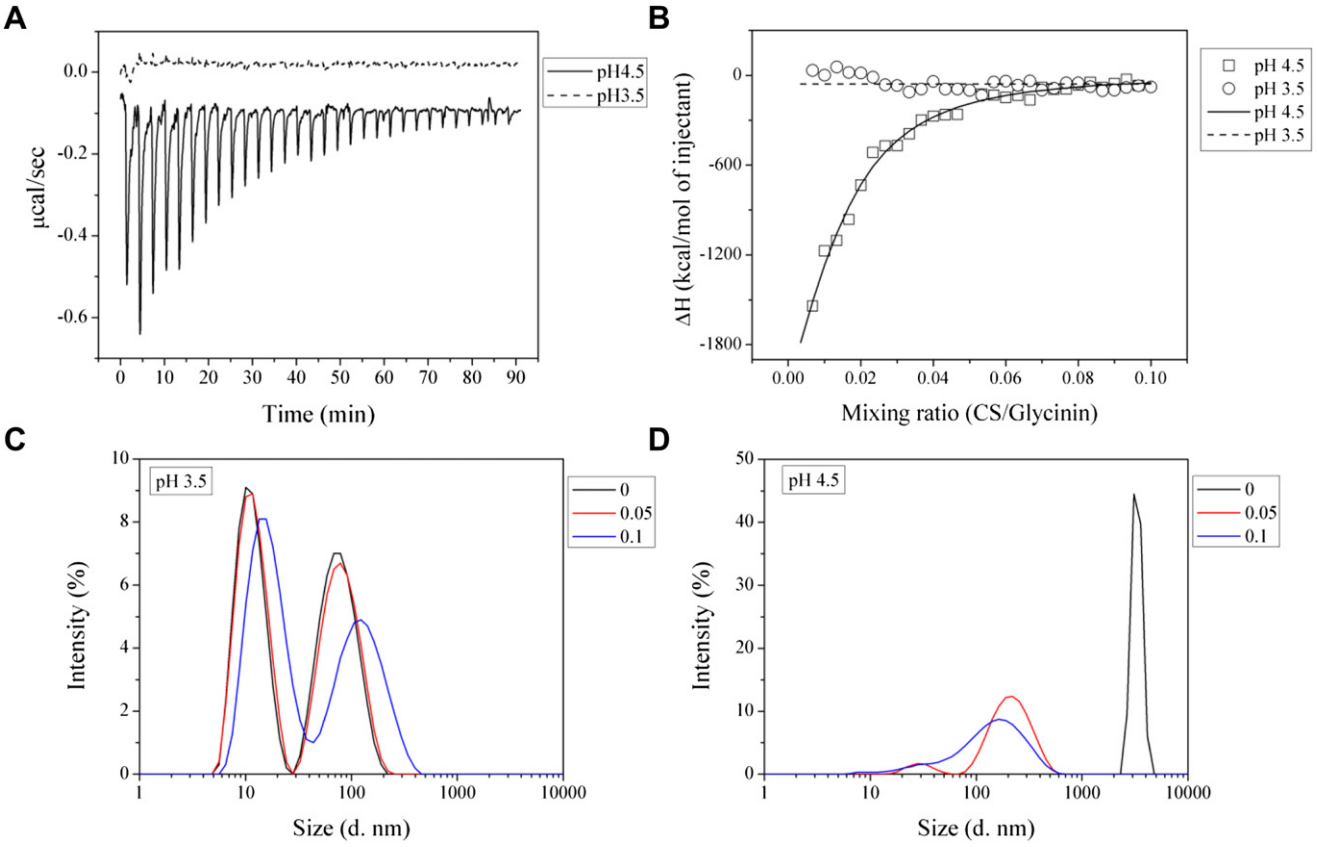

Fig. 3. The formation of glycinin/CS soluble complex at pH 3.5 and 4.5. Panel A and B are ITC data for the titration of glycinin solution with chitosan solution at pH 3.5 and 4.5. Panel A shows the raw data after baseline correction. Panel B shows the integrated heat of reaction (circle and square) and the best–fit curve (solid line and dashed line). Panel C and D are size distribution of glycinin/CS mixtures (CS/Glycinin mixing ratio of 0.05 and 0.1) and glycinin at pH 3.5 and 4.5.

exothermic heat of −1540.93 kcal/mol and then dropped gradually to the heat of dilution ΔH ≈ −26.93 kcal/mol (Fig. 3B). In addition, the heat effect of complex formation kept decreasing during the titration until the CS/Glycinin mixing ratio reached 0.10. This result suggested that, at this ratio, the binding was probably complete and glycinin was saturated with chitosan. Glycinin was partly negatively charged at pH 4.5, which was close to its isoelectric point, while chitosan was positively charged. Therefore, chitosan could bind to glycinin due to electrostatic attraction. These results can be proved by many previous studies on milk protein and chitosan (Guzey et al., 2006; Souza et al., 2009, 2011).

Fig. 3CD shows the size distribution of glycinin and glycinin/CS mixture (CS/Glycinin, 0.05 and 0.1) at pHs 3.5 and 4.5. At pH 3.5, glycinin/CS mixture exhibited the similar size distribution with glycinin, indicating that little attraction existed between glycinin and chitosan (Fig. 3C). At pH 4.5, the peak of size distribution changed from 3091 nm (glycinin) to 164.2 nm (glycinin/CS soluble complex at mixing ratio of 0.1). Without complexation with other polymers, proteins usually tend to aggregate at pHs close their to pIs. The formation of glycinin/CS complex inhibited the protein/protein aggregation, because of the existence of highly charged polysaccharide chains. The results of ITC and size distribution illuminated that complex formed at pH 4.5 and saturated at mixing ratio = 0.1, showing a maximum size distribution at 164.2 nm. These kinds of complexes were still soluble and highly charged (27.95 ± 0.85 mV, data not shown) due to the partial negative charge of carboxyl groups in glycinin molecules, which could interact with chitosan between parts of the opposite charge groups.

3.2. Dynamic interfacial adsorption

The dynamic surface pressures (π) of glycinin adsorbed films at the oil–water interface with different chitosan concentrations in the bulk phase are presented in Fig. 4. As shown in Fig. 4A, π values increased with adsorption time, which can be associated with the protein adsorption at the interface. The effect of chitosan on the time evolution of π depended on the concentration of polysaccharide. The presence of the chitosan in the bulk phase led to an increase of surface pressure when compared to the protein alone. CS/Glycinin mixing ratio of 0.1 showed the highest surface pressure after a long adsorption time (Fig. 4A).

From a kinetic point of view, protein adsorption to the oil–water interface has been described to occur in three main stages: (i) Diffusion from the bulk to the proximity of the interface; (ii) The adsorption and unfolding of the protein at the interface; (iii) The adsorption and rearrangement of protein segments at the fluid interface (Patino, Sanchez, Ortiz, Nino, & Anon, 2004). During the first step, at relatively low pressures when diffusion is the rate determining step, a modified form of the Ward and Tordai equation (Ward & Tordai, 1946) can be used to correlate the change in the surface pressure with time defined by Eq. (1).

$$\pi = 2C_0 KT(D\theta/3.14)^{1/2} \quad (1)$$

where C_0 is the concentration in the bulk phase, K is the Boltzmann constant, T is the absolute temperature, and D is the diffusion coefficient. If the diffusion of proteins at the interface controls the

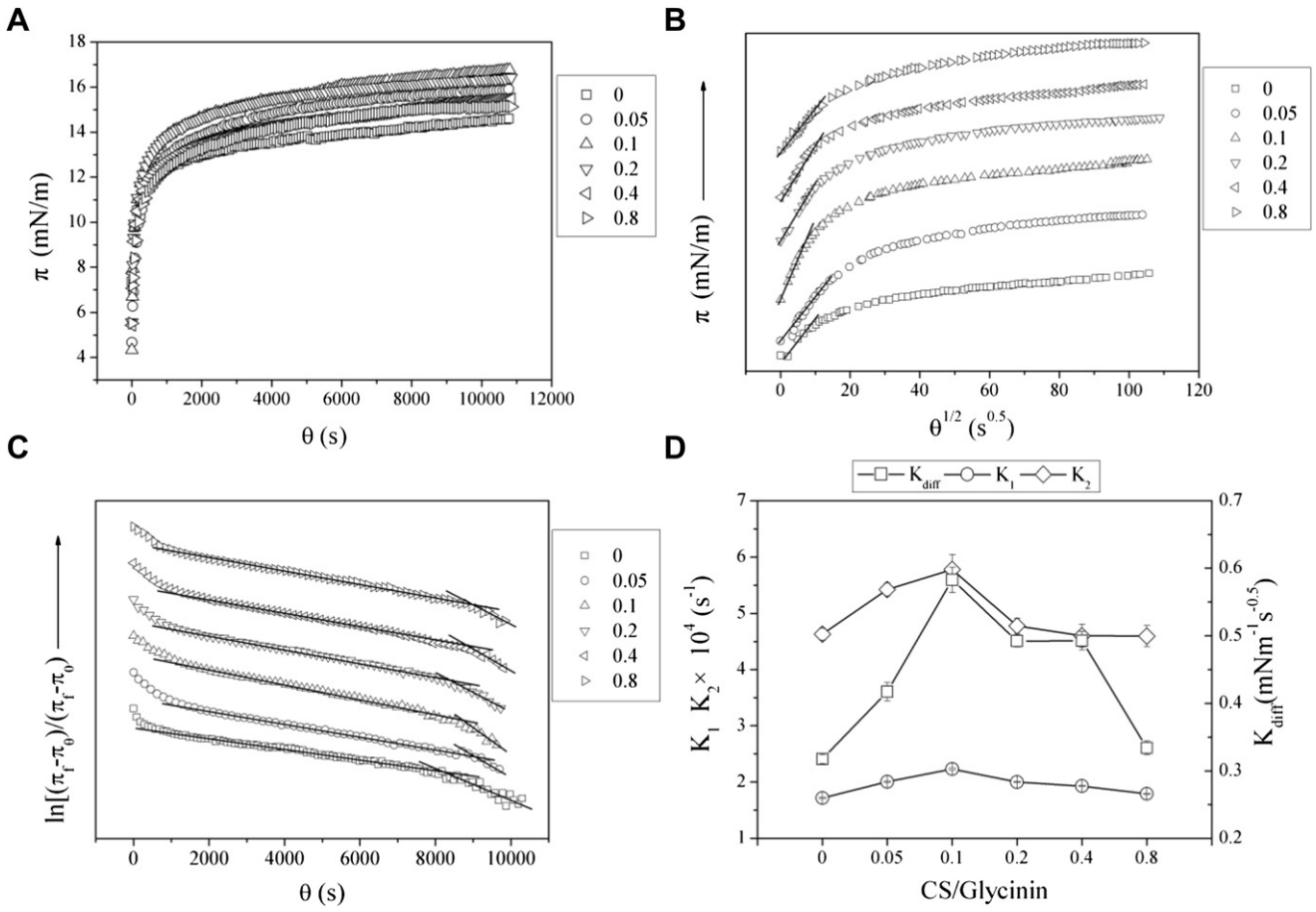

Fig. 4. Dynamic surface pressure of glycinin/CS mixture with different CS/Glycinin mixing ratio at oil–water interface. Panel A shows surface pressure (π) against adsorption time (θ). Panel B shows π against $\theta^{1/2}$ and best–fit curve of K_{diff} (soild line). Panel C shows $\ln(\pi_f-\pi_\theta)/(\pi_f-\pi_0)$ against θ and best–fit curve of K_1 and K_2 (solid line). Panel D shows slopes of K_{diff}, K_1 and K_2. Temperature = 25 °C, pH = 4.5.

adsorption process, a plot of π against $\theta^{1/2}$ will then be linear (Ward et al., 1946), and the slope of this plot will be the diffusion rate (K_{diff}).

The rates of unfolding and rearrangements of adsorbed protein molecules have been analyzed by a first-order equation (Graham & Phillips, 1979):

$$\ln\frac{\pi_f-\pi_\theta}{\pi_f-\pi_0} = -k_i\theta \quad (2)$$

where π_f, π_0 and π_θ are the surface pressures at the final adsorption time of each step, at the initial time, and at any time respectively, and k_i is the first-order rate constant. In practice, a plot of Eq. (2) usually yields two or more linear regions. The initial slope corresponds to a first-order rate constant of unfolding (K_1), while the second slope corresponds to rate constant of protein rearrangement (K_2).

The application of Eqs. (1) and (2) to glycinin adsorption with different chitosan concentrations at the oil–water interface are given in Fig. 4BC. As shown in Fig. 4B, all samples showed a good fit of the experimental data to the Eq. (1) at low surface pressures. Thus, it could be concluded that, during the initial period, the kinetics of glycinin and glycinin/CS mixtures adsorption at the oil–water interface were controlled by a diffusion mechanism. As shown in Fig. 4C, two linear regions in the plot of $\ln(\pi_f-\pi_\theta)/(\pi_f-\pi_0)$ against π were found in all experiments, indicating the existence of unfolding and rearrangement at the interface after the diffusion.

The slope derived from the π against $\theta^{1/2}$ and from $\ln(\pi_f-\pi_\theta)/(\pi_f-\pi_0)$ against π are reported in Fig. 4D. It can be seen that the K_{diff}, K_1 and K_2 of glycinin (0.32 mNm^{-1} $s^{-0.5}$, 1.72 E–4 s^{-1} and 4.63 E–4 s^{-1}) increased significantly at CS/Glycinin mixing ratio of 0.1 (0.58 mNm^{-1} $s^{-0.5}$, 2.23 E–4 $s^{-1}$and 5.78 E–4 s^{-1}) and showed almost no difference with mixing ratio of 0.8 (0.33 mNm^{-1} $s^{-0.5}$,

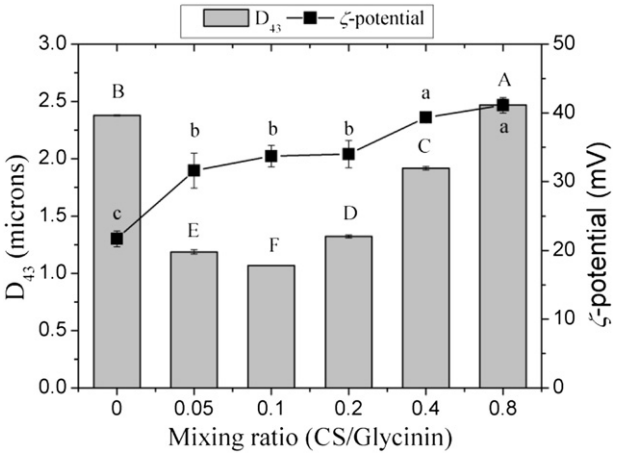

Fig. 5. Effect of CS/Glycinin mixing ratio on (A) ζ-potential and (B) droplet size (D_{43}) of glycinin/CS mixed emulsions at pH 4.5.

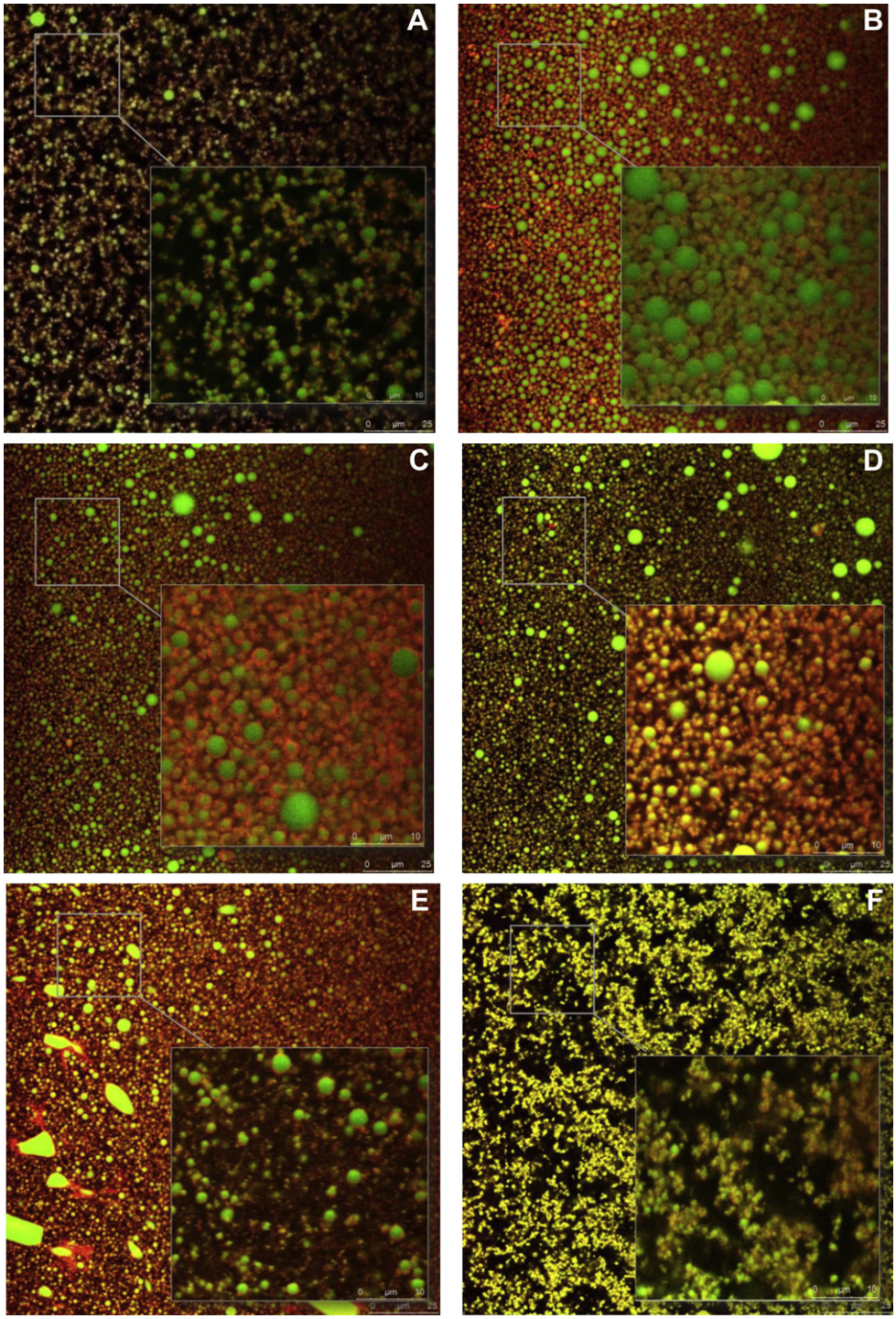

Fig. 6. CLSM of glycinin/CS mixed emulsions at pH 4.5 (A–F, 0, 0.05, 0.1, 0.2, 0.4 and 0.8, CS/Glycinin). The small photomicrographs were 3 times magnification of big one.

1.80 E−4 $s^{-1}$and 4.59 E−4 s^{-1}), respectively. A plausible explanation for this was that: (i) Glycinin tended to aggregate via hydrophobic interaction due to the reduction of electrostatic repulsion at pH 4.5. As a result of aggregation, glycinin showed lowest diffusion, unfolding and rearrangement coefficient at oil–water interface (Fig. 4D). Patino et al. (2004) reported similar results by using soy globulin at air–water interface. (ii) When glycinin adsorbed at the interface in the presence of suitable amount of chitosan, the glycinin/CS complex formed via electrostatic interaction inhibited the aggregate of glycinin. Probably because of the decreased particle size and increased hydrophobic residues, glycinin/CS complex exhibited improved property in diffusion, unfolding and rearrangement at interface. As a hydrophilic polysaccharide, chitosan is not considered to be surface active agents (Nyström, Kjøniksen, & Iversen, 1999), and the modification of surface properties of adsorbed or spread glycinin films suggested the participation of chitosan at the interface by a complexation mechanism (Martinez, Sanchez, Ruiz-Henestrosa, Patino, & Pilosof, 2007; Patino & Pilosof, 2011). Similar results of cooperative adsorption between WPI and chitosan was reported by Speiciene, Guilmineau, Kulozik, and

Leskauskaite (2007). (iii) However, the presence of excessive chitosan in the aqueous phase produced a decrease in K_{diff}, K_1 and K_2 value (Fig. 4D). This behavior may probably be explained by protein adsorption resistance due to the steric repulsion (Liu, Zhao, et al., 2011) by surplus chitosan (mixtures showed enhanced viscosity with chitosan increase, data not shown).

From the result of surface pressure, it can be assumed that the formation of soluble complex between chitosan and glycinin improved the interfacial adsorption of glycinin at pH 4.5. After glycinin was saturated with chitosan, however, cooperative adsorption was probably inhibited by the surplus chitosan. In other words, the cooperative effect of chitosan on interfacial adsorption of glycinin was dependent on the ratio of their concentrations.

3.3. Mixed emulsion

The ζ-potentials and sizes of mixed emulsions were investigated as a function of mixing ratio at pH 4.5 (Fig. 5). Fig. 5 showed that the ζ-potential of emulsion increased as the mixing ratio increased from 0 to 0.8. Concomitantly, the droplet size (D_{43}) decreased as the mixing ratio from 0 to 0.1 and then increased at higher chitosan concentration. This phenomenon might be associated with the fact that the emulsion with or without chitosan had different electrostatic repulsions between droplets at such pH. More importantly, such an effect may also be attributed to an increase in viscosity and surface activity of a continuous phase caused by the addition of chitosan, as shown previously. It was notable that the droplet size increased significantly at high chitosan concentrations, even if the ζ-potential was as high as that at low chitosan concentrations. It was probably due to the effect of depletion flocculation cause by surplus chitosan in the continuous phase (As shown in Fig. 3).

The formation of droplets with different sizes upon the addition of chitosan was confirmed by CLSM of emulsions in Fig. 6. In the present work, Nile blue–Nile red mixed fluorescence dye was applied to indicate the protein phase (excitation at 633 nm; red color) and oil phase (excitation at 488 nm; green color). In addition, the magnification coefficient of the smaller photomicrographs were 3 times that of the bigger ones. Fig. 6 indicated that the emulsions exhibited remarkable differences of microstructure depending on the mixing ratio. Compared with the control emulsion, the samples with mixing ratios of 0.05–0.2 had a homogeneous microstructure. The depletion flocculation, however, was clearly observed at highest chitosan concentration.

The stability of the emulsions were also investigated for 60 days storage (4 °C). The ζ-potential of all samples decreased gradually (Fig. 7A). Fig. 7B showed that the emulsion prepared by glycinin alone was relatively unstable, and that the D_{43} of the emulsions with mixing ratio of 0.4 and 0.8 were even greater than that of the control. As mentioned before, this result was probably due to the enhancement of depletion flocculation caused by the long-term storage. The emulsions with mixing ratios of 0.05 and 0.1 showed slight increase in D_{43} after storage, and that with a ratio of 0.2 exhibited highest stability.

The results above suggested that the interfacial coadsorption of chitosan with glycinin achieved saturation at appropriate mixing ratios. In the previous research on protein/CS emulsions, interfacial electrostatics, steric stabilizing, bridging and depletion flocculation mechanisms were often used to explain for the stability mechanisms of the mixed system (Laplante et al., 2005ab, 2006; Hong et al., 2007). Typically, the stability of emulsion was the equilibrium between repulsive interactions (electrostatic and steric) and attractive interactions (van der Waals and depletion) of the droplets. The instability of control emulsion was attributed to the aggregation of glycinin caused by the low net electrical charge near its pI. The addition of chitosan led to a high ζ-potential, high viscosity and high interfacial activity of continuous phase (as shown in Fig. 4), thus favoring the coadsorption at o/w interface. When the mixing ratio exceeded an appropriate value, however, emulsion became unstable because the depletion flocculation occurred in the presence of excessive chitosan. This phenomenon corresponded well to the interfacial adsorption of soluble complex. In one word, the stability emulsion could be promoted by interfacial coadsorption between glycinin and chitosan only at mixing ratio region which soluble complex formed without excessive chitosan.

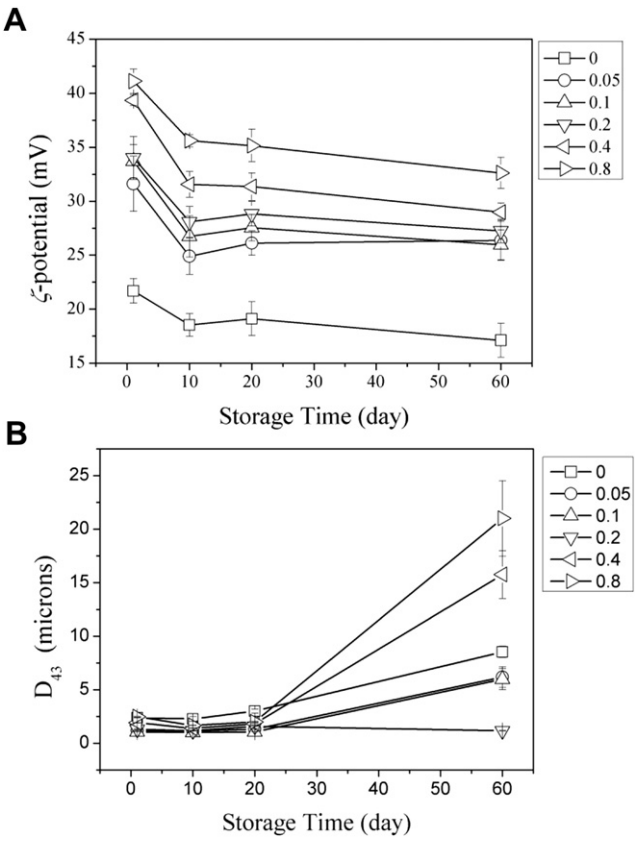

Fig. 7. Storage stability of glycinin/CS mixed emulsions with different CS/Glycinin mixing ratio at pH 4.5. (A) ζ-potential against storage time, (B) droplet size (D_{43}) against storage time.

4. Conclusion

The objective of this study was to examine the formation and dynamic interfacial adsorption of glycinin/CS soluble complex. The formation of glycinin/CS complex was electrostatic dependent at detected pH. At pH 4.5, the formation of soluble complex achieved saturation at mixing ratio = 0.1, which was indicated by isothermal titration calorimetry. The complex formed under the above-mentioned conditions exhibited maximum size distribution at 164.2 nm. The interfacial adsorption (oil–water interface) of glycinin was improved when soluble complex formed. The stability of mixed emulsions stabilized by glycinin/CS soluble complex was also investigated at pH 4.5. Improved emulsion stability was achieved at glycinin/CS ratio of 0.1–0.2, while excessive chitosan resulted in depletion flocculation. The equilibrium between repulsive interactions (electrostatic and steric) and attractive interactions (van der Waals and depletion) of the emulsion droplets was responsible for these results. This study can be an available reference for the utilization of chitosan in soybean-based food (e.g., soybean milk and soybean beverages).

Acknowledgments

This work is part of the research projects of Chinese National Natural Science Fund (Serial Number: 21076087 and 31130042, sponsored by the NSFC) and the Fundamental Research Funds for the Central Universities (SCUT, 2012ZZ0082).

References

Anal, A. K., Tobiassen, A., Flanagan, J., & Singh, H. (2008). Preparation and characterization of nanoparticles formed by chitosan-caseinate interactions. *Colloids and Surfaces B: Biointerfaces, 64*, 104–110.

Borges, O., Cordeiro-da-Silva, A., Romeijn, S. G., Amidi, M., de Sousa, A., Borchard, G., et al. (2006). Uptake studies in rat Peyer's patches, cytotoxicity and release studies of alginate coated chitosan nanoparticles for mucosal vaccination. *Journal of Control Release, 114*(3), 348–358.

Çakır, E., & Foegeding, E. A. (2011). Combining protein micro-phase separation and protein–polysaccharide segregative phase separation to produce gel structures. *Food Hydrocolloids, 25*(6), 1538–1546.

Caseli, L., Masui, D. C., Furriel, R. P. M., Leone, F. A., & Zaniquelli, M. E. D. (2005). Adsorption kinetics and dilatational rheological studies for the soluble and anchored forms of alkaline phosphatase at the air/water interface. *Journal of the Brazilian Chemical Society, 16*(5), 969–977.

Dickinson, E. (2008). Interfacial structure and stability of food emulsions as affected by protein-polysaccharide interactions. *Soft Matter, 4*(5), 932.

Duncan, D. B. (1955). Multiple range and multiple F test. *Biometrics, 11*, 1–42.

Elmer, C., Karaca, A. C., Low, N. H., & Nickerson, M. T. (2011). Complex coacervation in pea protein isolate–chitosan mixtures. *Food Research International, 44*(5), 1441–1446.

Farouk, M. M., Frost, D. A., Krsinic, G., & Wu, G. (2011). Phase behaviour, rheology and microstructure of mixture of meat proteins and kappa and iota carrageenans. *Food Hydrocolloids, 25*(6), 1627–1636.

Gharsallaoui, A., Yamauchi, K., Chambin, O., Cases, E., & Saurel, R. (2010). Effect of high methoxyl pectin on pea protein in aqueous solution and at oil/water interface. *Carbohydrate Polymers, 80*(3), 817–827.

Graham, D. E., & Phillips, M. C. (1979). Proteins at liquid interfaces. III. Kinetic of adsorption and surface denaturation. *Journal of Colloids and Interface Science, 70*, 427–439.

Guzey, D., & McClements, D. J. (2006). Characterization of beta-lactoglobulin-chitosan interactions in aqueous solutions: a calorimetry, light scattering, electrophoretic mobility and solubility study. *Food Hydrocolloids, 20*(1), 124–131.

Hong, Y. H., & McClements, D. J. (2007). Formation of hydrogel particles by thermal treatment of beta-lactoglobulin-chitosan complexes. *Journal of Agricultural and Food Chemistry, 55*(14), 5653–5660.

Jourdain, L., Leser, M. E., Schmitt, C., Michel, M., & Dickinson, E. (2008). Stability of emulsions containing sodium caseinate and dextran sulfate: relationship to complexation in solution. *Food Hydrocolloids, 22*(4), 647–659.

Laplante, S., Turgeon, S. L., & Paquin, P. (2005a). Effect of pH, ionic strength, and composition on emulsion stabilising properties of chitosan in a model system containing whey protein isolate. *Food Hydrocolloids, 19*(4), 721–729.

Laplante, S., Turgeon, S. L., & Paquin, P. (2005b). Emulsion stabilizing properties of various chitosans in the presence of whey protein isolate. *Carbohydrate Polymers, 59*(4), 425–434.

Laplante, S., Turgeon, S. L., & Paquin, P. (2006). Emulsion-stabilizing properties of chitosan in the presence of whey protein isolate: effect of the mixture ratio, ionic strength and pH. *Carbohydrate Polymers, 65*(4), 479–487.

Liu, C., Yang, X. Q., Lin, M. G., Zhao, R. Y., Tang, C. H., Luo, L., et al. (2011). Complex coacervation of chitosan and soy globulins in aqueous solution: a electrophoretic mobility and light scattering study. *International Journal of Food Science and Technology, 46*, 1363–1369.

Liu, L. Y., Zhao, Q. Z., Liu, T. X., Kong, J., Long, Z., & Zhao, M. M. (2012). Sodium caseinate/carboxymethylcellulose interactions at oil-water interface: relationship to emulsion stability. *Food Chemistry, 132*(4), 1822–1829.

Liu, L. Y., Zhao, Q. Z., Liu, T. X., & Zhao, M. M. (2011). Dynamic surface pressure and dilatational viscoelasticity of sodium caseinate/xanthan gum mixtures at the oil-water interface. *Food Hydrocolloids, 25*(5), 921–927.

Martin, A. H., Bos, M. A., & van Vliet, T. (2002). Interfacial rheological properties and conformational aspects of soy glycinin at the air/water interface. *Food Hydrocolloids, 16*(1), 63–71.

Martinez, K. D., Sanchez, C. C., Ruiz-Henestrosa, V. P., Patino, J. M. R., & Pilosof, A. M. R. (2007). Soy protein-polysaccharides interactions at the air-water interface. *Food Hydrocolloids, 21*(5–6), 804–812.

Mounsey, J. S., O'Kennedy, B. T., Fenelon, M. A., & Brodkorb, A. (2008). The effect of heating on beta-lactoglobulin-chitosan mixtures as influenced by pH and ionic strength. *Food Hydrocolloids, 22*(1), 65–73.

Nagano, T., Hirotsuka, M., Mori, H., Kohyama, K., & Nishinari, K. (1992). Dynamic viscoelastic study on the gelation of 7 S globulin from soybeans. *Journal of Agricultural and Food Chemistry, 40*(6), 941–944.

No, H. K., Park, N. Y., Lee, S. H., & Meyers, S. P. (2002). Antibacterial activity of chitosans and chitosan oligomers with different molecular weights. *International Journal of Food Microbiology, 74*, 65–72.

Nyström, B., Kjøniksen, A. L., & Iversen, C. (1999). Characterization of association phenomena in aqueous systems of chitosan of different hydrophobicity. *Advances in Colloid and Interface Science, 79*, 81–103.

Patino, J. M. R., & Pilosof, A. M. R. (2011). Protein-polysaccharide interactions at fluid interfaces. *Food Hydrocolloids, 25*(8), 1925–1937.

Patino, J. M. R., Sanchez, C. C., Ortiz, S. E. M., Nino, M. R. R., & Anon, M. C. (2004). Adsorption of soy globulin films at the air-water interface. *Industrial & Engineering Chemistry Research, 43*(7), 1681–1689.

Schmitt, C., & Turgeon, S. L. (2011). Protein/polysaccharide complexes and coacervates in food systems. *Advances in Colloid and Interface Science, 167*(1–2), 63–70.

Souza, H. K. S., Bai, G., Gonçalves, M.d. P., & Bastos, M. (2009). Whey protein isolate-chitosan interactions: a calorimetric and spectroscopy study. *Thermochimica Acta, 495*(1–2), 108–114.

Souza, H. K. S., Gonçalves, M.d. P., & Gómez, J. (2011). Effect of chitosan degradation on its interaction with beta-lactoglobulin. *Biomacromolecules, 12*(4), 1015–1023.

Speiciene, V., Guilmineau, F., Kulozik, U., & Leskauskaite, D. (2007). The effect of chitosan on the properties of emulsions stabilized by whey proteins. *Food Chemistry, 102*(4), 1048–1054.

Staswick, P. E., Hermodson, M. A., & Nielsen, N. C. (1981). Identification of the acidic and basic subunit complexes of glycinin. *The Journal of Biological Chemistry, 256*, 8752–8755.

Takeuchi, T., Morita, K., Saito, T., Kugimiya, W., & Fukamizo, T. (2006). Chitosan–soyprotein interaction as determined by thermal unfolding experiments. *Bioscience Biotechnology Biochemistry, 70*(7), 1786–1789.

Turgeon, S. L., Schmitt, C., & Sanchez, C. (2007). Protein–polysaccharide complexes and coacervates. *Current Opinion in Colloid & Interface Science, 12*(4–5), 166–178.

van Vliet, T., Martin, A. H., & Bos, M. A. (2002). Gelation and interfacial behaviour of vegetable proteins. *Current Opinion in Colloid & Interface Science, 7*, 462–468.

Vardhanabhuti, B., Yucel, U., Coupland, J. N., & Foegeding, E. A. (2009). Interactions between β-lactoglobulin and dextran sulfate at near neutral pH and their effect on thermal stability. *Food Hydrocolloids, 23*(6), 1511–1520.

Ward, A. F. H., & Tordai, L. (1946). time dependence of boundary tensions of solutions. I. The role of diffusion in time effects. *Journal of Chemical Physics, 14*, 353–361.

Weinbreck, F., de Vries, R., Schrooyen, P., & de Kruif, C. G. (2003). Complex coacervation of whey proteins and gum arabic. *Biomacromolecules, 4*, 293–303.

Ye, A. Q., Flanagan, J., & Singh, H. (2006). Formation of stable nanoparticles via electrostatic complexation between sodium caseinate and gum arabic. *Biopolymers, 82*, 121–133.

Zhu, J. H., Yang, X. Q., Ahmad, I., Li, L., Wang, X. Y., & Liu, C. (2008). Rheological properties of κ-carrageenan and soybean glycinin mixed gels. *Food Research International, 41*(3), 219–228.